

Interaction of neutrons with even- A tin isotopes.I. Total cross sections for $E_n = 0.3 - 5.0$ MeVR. W. Harper,* T. W. Godfrey,[†] and J. L. Weil*Department of Physics and Astronomy, University of Kentucky, Lexington, Kentucky 40506*

(Received 18 January 1982)

The neutron total cross sections of $^{116,118,120,122,124}\text{Sn}$ have been measured in the energy range $E_n = 0.3 - 5.0$ MeV with an energy resolution ranging from 100 keV at 0.3 MeV to 30 keV at 5 MeV. The measurements were made in good geometry using the time-of-flight method to reduce background effects, and the uncertainty in the cross sections ranges from 1.0% at low energy to 2.4% above 4 MeV. Unresolved fine structure can be seen in the cross sections of some of the isotopes below 1 MeV. Ignoring this fine structure, all the measured cross sections agree within 5% up to 2 MeV and 10% over the whole energy range with the cross section calculated from a complex potential whose real and imaginary well depths have the usual linear energy dependence, and also a neutron excess dependence. This potential was originally determined to fit the elastic scattering differential cross sections of these isotopes at a bombarding energy of 1 MeV.

<p>NUCLEAR REACTIONS $^{116,118,120,122,124}\text{Sn} + n$, $E_n = 0.3 - 5.0$ MeV; measured transmission, deduced σ_T, compared σ_T with optical model. Isotopically enriched samples, resolution 30–100 keV, neutron time of flight.</p>

I. INTRODUCTION

This paper is the first in a series reporting on the results of an experimental investigation into the neutron excess dependence of the optical potential parameters which describe neutron-nucleus scattering, both elastic and inelastic. Five even- A tin nuclides, $^{116,118,120,122,124}\text{Sn}$ were chosen for this study for three reasons. Firstly, this isotope set offers one of the largest ranges of the neutron excess parameter, $(N - Z)/A$, in the Periodic Table. Secondly, the well-known nuclear structure similarities for the isotopes of tin are as strong as or stronger than are found in any other element, leading one to expect the smallest perturbations of systematic neutron excess dependence by structural variations. The properties showing similarity include the low-lying energy level structure, shown in Fig. 1, the static quadrupole moments of the first excited states which are close to zero¹ for all five isotopes, and the quadrupole excitation parameters for the first excited states ($\beta_2 \cong 0.1$ for all five isotopes) determined both from Coulomb excitation² and from neutron and proton inelastic scattering at bombarding energies of 11 MeV,³ and 16 MeV,⁴ respectively. These

similarities between all five isotopes indicate that they should provide a satisfactory system for the study of the effects of adding successive pairs of neutrons to a nucleus. The third reason is the relatively large natural abundance of each of these isotopes, which results in sufficiently large separated isotope samples being available to do precision neutron scattering and total cross section experiments. The concurrence of these three factors make this isotope set a unique case for such an investigation.

Satchler⁵ reviewed the state of knowledge about the neutron excess dependence of the optical model potential in 1969, including the results of both global studies and studies of isotopic sequences. By then it was clear that for proton scattering there was a fairly well determined neutron excess dependence for the real potential and also a strong indication of a similar dependence in the surface imaginary potential. However, the poor precision of the neutron scattering data available at that time made it impossible to say whether the size of the neutron excess dependence was the same for the neutron and proton potentials.

Since then the precision of neutron scattering measurements has improved considerably, and there

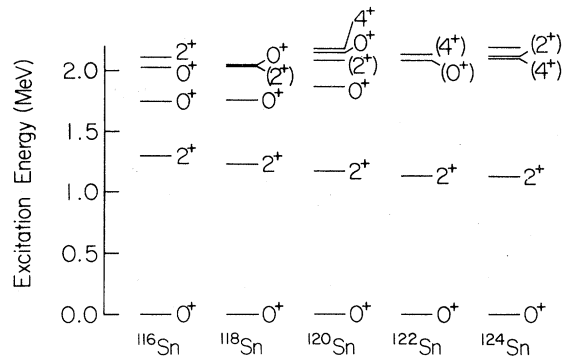


FIG. 1. Energy-level diagrams of the isotopes used in this study.

have been a number of studies published in recent years on the neutron excess dependence of the neutron optical potential. Included in these published works are global analyses for $24 \leq A \leq 209$ at $E_n = 11$ MeV,⁶ and for $40 \leq A \leq 208$ in the energy range $E_n = 7-26$ MeV.⁷ There have also been analyses of the neutron scattering from sequences of Se isotopes at $E_n = 6-8$ MeV,⁸ Mo isotopes for $E_n = 7-26$ MeV,⁹ and Sn isotopes for $E_n = 11$ and 24 MeV.¹⁰

In the series of papers of which this is the first, we will report on the neutron excess dependence of the neutron optical potential as determined by the scattering of neutrons in the energy range $E_n = 1-4$ MeV from a sequence of Sn isotopes. The incident neutron energies were chosen so as to strongly vary the number of open channels and look for the effect of this variation on the neutron excess dependence. Such a study could hardly have been done for proton scattering because of the large Coulomb barrier.

In the present work the total cross sections of $^{116}, ^{118}, ^{120}, ^{122}, ^{124}\text{Sn}$ have been measured by the transmission method using isotopically enriched samples. The availability of these samples,¹¹ each enriched to more than 90% in a given isotope, enabled a search for systematic cross section variations that could be correlated with the neutron excess. We have measured the total cross section of carbon at the same time as those of the tin isotopes as a check against systematic errors. Time-of-flight (TOF) methods were used to reduce background and improve precision. A preliminary report¹² of this work has appeared. This total cross section study was originally motivated by the need for a convenient and accurate means of normalizing low-energy neutron scattering differential cross sections measured in this laboratory at 1.0 and 1.63 MeV.¹³ It was found that using the measured total

cross sections for normalization resulted in a significant improvement in the precision of the scattering differential cross sections. The study was then extended in scope in order to compare to the neutron-excess dependent potential, as well as to make the cross sections available for others to use. The only previous total cross section measurements at these specific energies were on natural tin by Adair¹⁴ and by Miller *et al.*¹⁵ Almost all previous neutron total cross section measurements¹⁶ in the energy region studied here, 0.3 to 5.0 MeV, were also made with natural tin samples.

II. EXPERIMENTAL METHOD

The University of Kentucky Van de Graaff accelerator produced a pulsed proton beam with a pulse frequency of 2.0 MHz and a pulse duration of 8–10 ns. The protons passed through a 3.3×10^{-4} cm thick Mo foil and entered a cell 3.0 cm in length containing approximately 0.2 atm of tritium gas. Neutrons were produced by the $T(p,n)^3\text{He}$ reaction. The experiment was performed with good geometry using a forced-reflection neutron collimator,^{17,18} shown in Fig. 2, between the source and the attenuation sample. The collimator was designed for use with neutron energies below 2 MeV, but was found to reduce the background even at 5 MeV. The distance from the source to the sample was 87 cm and the distance from source to detector was 290 cm. This extended geometry with close collimation made the alignment of the system rather critical (the sample axis had to be within 1.0 mm of the source to detector axis) but was chosen over a more conventional compact, open geometry because it reduced the neutron background and reduced in-scattering corrections to about one part in 10^6 . The

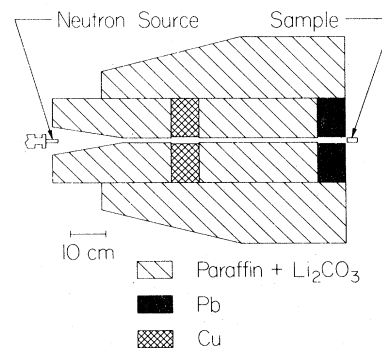


FIG. 2. The forced-reflection neutron collimator, cut-away view.

TABLE I. Composition and dimensions of scattering samples.

Sample	Isotopic composition (atomic %)										Mass (g)	Diameter (cm)	Length (cm)
	¹¹² Sn	¹¹⁴ Sn	¹¹⁵ Sn	¹¹⁶ Sn	¹¹⁷ Sn	¹¹⁸ Sn	¹¹⁹ Sn	¹²⁰ Sn	¹²² Sn	¹²⁴ Sn			
¹¹⁶ Sn	<0.01	0.03	0.06	95.74	1.02	1.49	0.32	1.06	0.13	0.15	42.610	1.590	3.020
¹¹⁸ Sn	<0.03	<0.03	<0.03	0.39	0.40	97.15	0.64	1.20	0.10	0.12	43.069	1.590	3.002
¹²⁰ Sn	<0.05	<0.05	<0.05	0.20	0.12	0.50	0.39	98.39	0.15	0.26	44.975	1.590	3.080
¹²² Sn	<0.02	<0.02	<0.02	1.01	0.58	1.91	0.77	3.75	90.80	1.16	29.198	1.590	1.975
¹²⁴ Sn	0.05	0.05	0.05	0.92	0.49	1.60	0.58	2.36	0.77	93.28	45.902	1.590	3.054

large source-detector separation also had the advantage of giving a good signal-to-background ratio because of the use of the TOF method of neutron spectroscopy.

The neutron detector was a 3.25 cm diameter by 2.54 cm long cylinder of NE218 liquid scintillator coupled to a 56 AVP photomultiplier. The electronic setup for the TOF neutron detector was essentially the same as that shown in Ref. 13. At bombarding energies greater than 300 keV, the detector was biased at a neutron energy of 300 keV, corresponding to the valley of the spectrum of the ²⁴¹Am γ ray, and at 300 keV, the bias was lowered appropriately. The detector was mounted in a large Li₂CO₃-loaded paraffin shield to reduce the background from room-scattered neutrons. This is the main or rear shield shown in Ref. 19.

The absorption samples were set on a low-mass plastic cradle which could be moved vertically and horizontally with fine-pitch screws for precision positioning. The samples were approximately one-third mole apiece, and their dimensions and composition are given in Table I. The symmetry axes of the collimator, sample, detector shield, and detector were aligned optically with the proton beam entering the gas cell, and the alignment was checked by translating the samples horizontally and vertically across the collimator axis while measuring the neutron transmission. The neutron monitor was a long counter placed 1 m from the tritium cell at an angle of about 100° to the beam. The proton beam current incident on the tritium cell was integrated and provided a second monitor of the neutron flux. Details of the University of Kentucky neutron TOF system may be found elsewhere.^{13,19,20}

TOF spectra of the unattenuated beam as well as of the neutrons transmitted by the tin and carbon samples were measured at energy intervals of 50–300 keV, and typical examples of such spectra are shown in Fig. 3. With the usual gas pressure of 0.2 atm, neutron energy spreads ranged from 100

keV at 0.3 MeV neutron energy to 30 keV at 4.5 MeV. Runs lasted 3–10 min with proton beams of 1–2 μ a. TOF spectra were accumulated in the memory of a PDP/8-I computer. Typical sample-in and sample-out neutron peaks contained 3×10^4 and 6×10^4 counts, respectively. The time-uncorrelated background in the region of the peak was about 4% of the net yield, and was subtracted. Dead time corrections of 1–5% were applied. In-scattering and hardening effects were calculated to be $\leq 0.1\%$, and hence were neglected as insignificant. Neutron transmissions of the samples were used to calculate total cross sections.

The experimental results were checked in a variety of ways. Many points were repeated several times, sometimes with different experimental conditions. At several energies, a 28 cm long by 2.54 cm diameter Cu "shadow bar" was suspended along the transmission axis at the exit port of the collimator, and the measured transmission indicated that no more than 0.1% of the flux detected without the bar was due to off-axis neutrons. Occasionally the tritium was removed from the cell and replaced with air, and a spectrum taken. If a significant number of neutrons produced from tritium absorbed into the tantalum cell liner was detected, the cell was taken apart and the liner and foil were replaced. A TOF spectrum with an acceptable background due to absorbed tritium is shown in Fig. 3. Finally, comparing the measured carbon total cross section with accurate results of other total cross section experiments^{21,22} provided a check on the whole measurement technique.

III. EXPERIMENTAL RESULTS

Figure 4 shows all the data taken for ¹²⁰Sn. Somewhat more data was taken for ¹²⁰Sn and ¹²⁴Sn than for the other samples, and the ¹²⁰Sn cross section is shown because it is typical, and because the

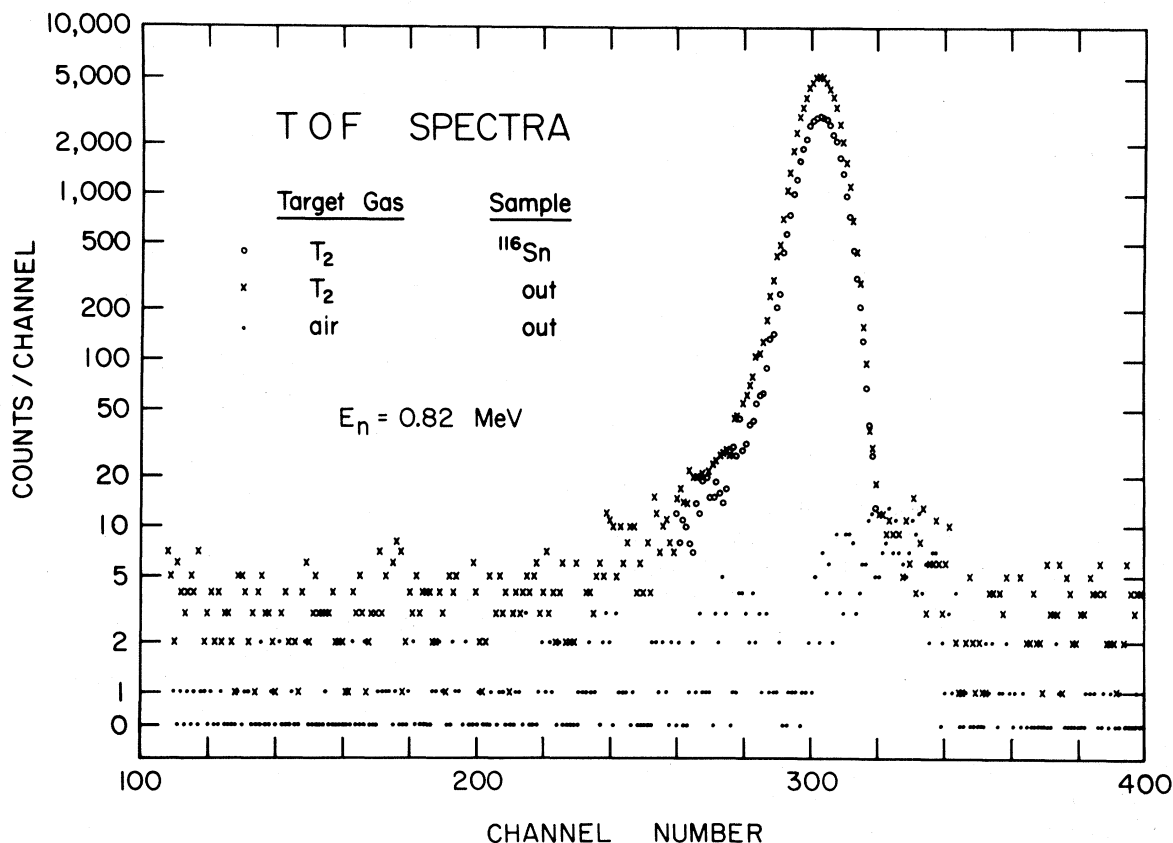


FIG. 3. Time-of-flight spectra of 0.81 MeV neutrons taken with and without an absorption sample. The third spectrum was measured with air in the gas cell in order to measure the background from absorbed tritium.

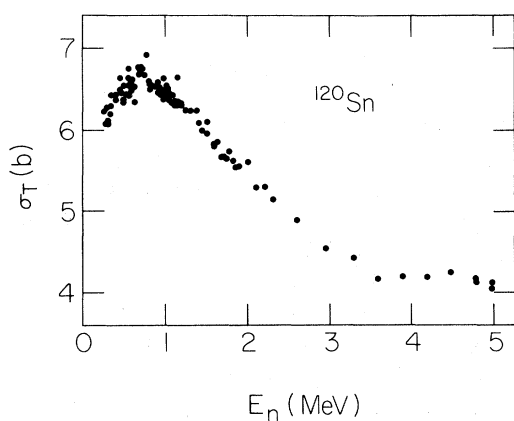


FIG. 4. Unsmoothed cross sections for ¹²⁰Sn. Some of these points were taken under experimental conditions different from those described in the text, and hence were not included in the smoothed and averaged data presented in Fig. 6.

fluctuations (discussed in Sec. IV) are clearly evident in the large number of repeated data points.

In order to reduce the data to a convenient table of total cross sections versus bombarding energy, the cross sections for each Sn isotope and for carbon were averaged and smoothed as follows. In regions where data was taken at energy intervals of 50 keV or less, the average of the cross sections in the interval $E_n \pm 50 \text{ keV}$ was taken to represent the measured total cross section at E_n . This procedure was carried out at 50 keV intervals. Where the data points were more than 50 keV apart, the data at each bombarding energy were averaged, and this was taken to represent the cross section at that energy. This kind of averaging was consistent with the energy spread, and the smoothing is justified because, at a given energy, the fluctuations in the cross sections outside statistical expectations appeared to be random.

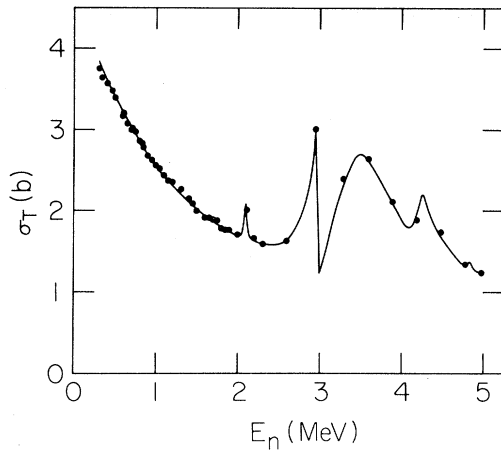


FIG. 5. The smoothed and averaged total cross section for carbon from the present work is given by the dots. The curve is drawn through the cross sections of Perey *et al.* (Ref. 21) below 0.55 MeV and through the cross sections of Schwartz *et al.* (Ref. 22) at higher energies.

Carbon total cross sections measured in the present work and smoothed in this same way are shown in Fig. 5. The curve is taken from Perey *et al.*²¹ below 0.55 MeV, and above this energy is from Schwartz *et al.*²² averaged over energy spreads appropriate to this experiment. The systematic uncertainties in the Perey and the Schwartz measurements are $+2.5\%$ and $\pm 1\%$, respectively. A smooth curve drawn through our energy-averaged cross section points for carbon below 2.0 MeV agrees with the measurements of Perey, but is in most cases just outside the stated $\pm 1\%$ uncertainty in the cross sections of Schwartz. Above 2.0 MeV, we do not have enough data to draw a curve which shows all the structure known to be present. Our cross sections in this region are within 0.05 b of those of Schwartz except for one data point at 4.2 MeV, which differs by 0.1 b. The average disagreement between our cross sections and those of Schwartz between 2.0 and 5.0 MeV is 1.6%.

The smoothed isotopic tin total cross sections are shown in Fig. 6. They are all similar in their general energy dependence, reaching a maximum between 500 and 900 keV, falling to about 4.1 b at 4 MeV, and then are relatively constant up to 5.0 MeV.

There are significant differences among the isotopes, however. The energy position of the cross section maximum increases with neutron excess except for ^{122}Sn , whose peak is at a lower energy than

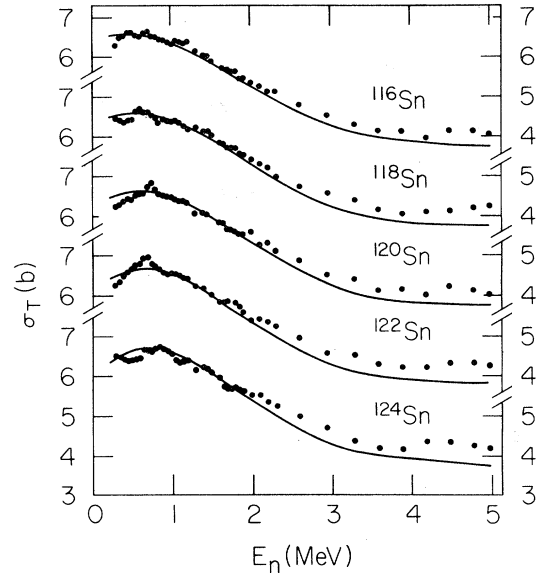


FIG. 6. The smoothed and averaged neutron total cross sections for five even- A tin isotopes. The curves are optical model calculations with a standard energy dependence, as discussed in Sec. VI.

that of ^{120}Sn . Also, the peak of the ^{122}Sn cross section is 0.3 b higher than that of the other isotopes. Some fine structure with width greater than or equal to the neutron energy spread was observed for all the isotopes and appears to become more prominent as A increases. The reproducibility of this fine structure was more thoroughly tested for ^{124}Sn and ^{122}Sn than for the other isotopes.

IV. UNCERTAINTIES

The only *known* contribution to the uncertainty in the cross sections that was significant was the counting statistics in the detected neutrons. The backgrounds did not contribute significantly to the statistical uncertainties, and uncertainties in the sample sizes are insignificant and, moreover, systematic. However, random fluctuations in the cross sections of both carbon and tin were two to three times larger than would be predicted by statistics alone, and much repeating of points and changing of experimental conditions did not reduce this fluctuation, nor lead to an understanding of the cause.

At bombarding energies below 2.3 MeV, where there were typically 5–10 data points per 100 keV interval, the 2–3% random fluctuations present in the raw data have been almost removed by the

smoothing and averaging process discussed in Sec. III. In this region we base our estimate of the uncertainty in the tin cross sections on the good agreement of our measured carbon cross section with accurate standards.^{21,22} Thus, we estimate the uncertainty below 2.3 MeV to be 1.0–1.8%. At higher bombarding energies there are so few data points that the averaging process had little effect on the magnitude of the fluctuations, and we base our estimated tin cross section uncertainty on the ± 0.1 b fluctuations. This is consistent with the carbon comparison since our carbon cross section differs from the standard by no more than 0.1 b. Thus, we estimate the uncertainty in the energy range 2.3–5.0 MeV to be 2.0–2.4%.

V. DISCUSSION AND COMPARISON WITH OTHER MEASUREMENTS

Previous measurements^{23,24} of natural tin total cross sections in the region 200–700 keV with energy spreads of 5–10 keV have revealed structures with a width of 25–100 keV and an amplitude of 10–15% of the total cross section. One would expect to observe more structure with separated isotopes than with natural tin, but in our experiment any increase was obscured by our large energy spread. The structure we do observe is not inconsistent with earlier measurements on natural tin. The fact that ^{124}Sn shows more structure than the other isotopes may be due to clusters of narrow resonances in the cross section. High-resolution transmission measurements by Harvey²⁵ show that of these isotopes, ^{124}Sn is considerably more resonant than the others for neutron energies up to 400 keV, the highest energy studied by him.

A weighted average of the isotopic cross sections, intended to synthesize the natural tin total cross section, has been calculated and is shown in Fig. 7. Any comparison of this with measurements on natural tin is somewhat open to question, however, because of the lack of data on the total cross sections of the odd-*A* isotopes, which comprise about 17% of natural tin. We have assumed the total cross sections of the tin isotopes at each energy to be a linear function of neutron number for the purpose of making this comparison with natural tin total cross sections.

We have averaged the high-resolution tin cross section data of Seth²⁴ and of Whalen²³ over 100-keV intervals to compare with our weighted average. As can be seen in Fig. 7, our average is 3–6% below Whalen's cross section and from 1% below to

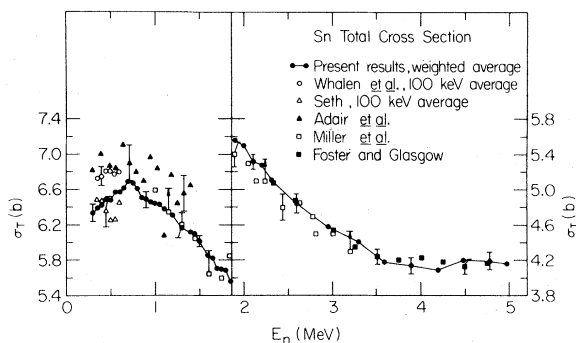


FIG. 7. The neutron total cross section of natural tin, synthesized from the isotopic cross sections by means of a weighted average, is indicated by the dots. The other symbols represent results for natural tin taken from the literature.

5% above that of Seth. Seth's measurements indicate a dip in the cross sections at 550 keV that is not present either in our results or in those of Whalen. Overall, however, our cross sections agree with those of Seth within mutual uncertainties, but are consistently outside the mutual uncertainty when compared to those of Whalen.

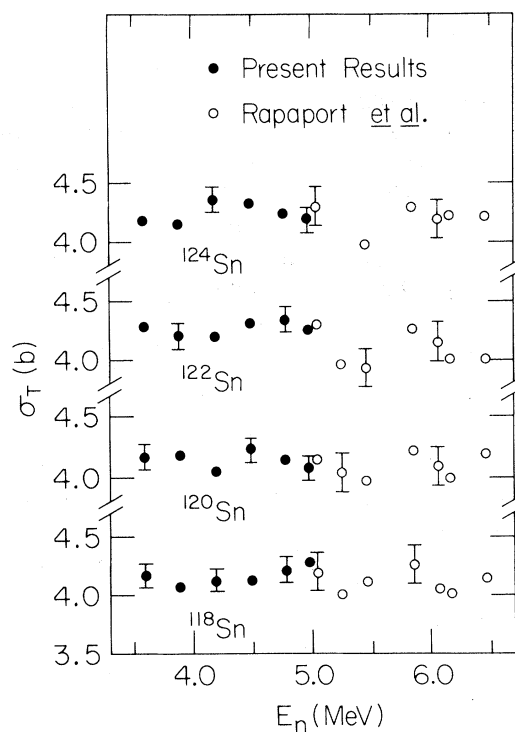


FIG. 8. Isotopic total cross sections measured in this experiment compared to the results of Rapaport *et al.* (Ref. 10).

Measurements of the natural tin cross section with energy spreads comparable to ours are reported by Miller *et al.*¹⁵ and Adair¹⁴ between 0.2 and 3.2 MeV using BF₃ detectors, and by Foster and Glasgow²⁶ above 2.2 MeV using the time-of-flight technique. Our synthesized natural tin cross sections disagree quite badly with the data of Adair, the worst disagreement being 0.4 b. The arrows indicate the change that would occur in Miller's cross section if they had used the recently measured¹³ forward-peaked differential cross section in making the inscattering correction instead of assuming that the scattering angular distribution is isotropic. This change improves agreement with Miller above 1.5 MeV but makes the agreement worse at lower energies, and also leads to worse agreement with Adair. Our data agree with those of Foster and Glasgow within uncertainties.

Above 5.0 MeV, Rapaport *et al.*¹⁰ have measured the isotopic total cross sections of tin with four of the five scattering samples used in our experiment. As can be seen in Fig. 8, their cross sections agree quite well with the data presented here.

VI. THEORETICAL ANALYSIS

The shift of the maximum in the total cross section to higher energies as neutron excess increases can be modeled by an optical potential²⁷ with neutron-excess dependent real and imaginary well depths. The potential used here is a spherical optical model (SOM) and is the same potential that fit 1.0 MeV elastic scattering differential cross sections for these isotopes,¹³ with the addition of an energy dependence for the real and imaginary well depths taken from the global analysis of Wilmore and Hodgson.²⁸ The complex potential was of the standard form

$$V(r) = -Vf(r) - iWg(r) - U_{so}h(r)\vec{l} \cdot \vec{\sigma},$$

where the real potential has a Woods-Saxon form, the imaginary potential has a Woods-Saxon derivative form, and the spin-orbit potential is real with a Thomas form, i.e.,

$$f(r) = [1 + \exp((r - r_0 A^{1/3})/a)]^{-1},$$

$$g(r) = 4a' \left| \frac{d}{dr} \left\{ [1 + \exp((r - r'_0 A^{1/3})/a')]^{-1} \right\} \right|,$$

$$h(r) = \left[\frac{\hbar}{m_\pi c} \right]^2 \frac{1}{r} \left| \frac{d}{dr} f(r) \right|.$$

The geometrical parameters used were

$$r_0 = 1.26 \text{ fm},$$

$$a = 0.58 \text{ fm},$$

$$r'_0 = 1.26 \text{ fm},$$

$$a' = 0.40 \text{ fm}.$$

The well depths in MeV were parametrized, for $R = r_0 A^{1/3}$, as

$$V = 53.0 - 30.5 \left[\frac{N-Z}{A} \right] - 0.27E_n,$$

$$W = 13.6 - 46.6 \left[\frac{N-Z}{A} \right] - 0.053E_n,$$

$$U_{so} = 5.5.$$

The calculated cross sections are compared with experiment in Fig. 6. The gross structure and magnitude of the experimental cross sections from 0.3 to 2.0 MeV and, in particular, the dependence of the energy of the cross section maximum on mass number, agree quite well with this model. At higher energies, however, the cross sections predicted by this optical potential are lower than the measurements by 0.2–0.4 b. This is not surprising in view of the fact that the potential was constructed to fit the 1.0 MeV differential scattering cross sections, and that no search was made on the energy dependence.

VII. CONCLUSIONS

The even- A isotopic tin cross sections from 0.3 to 5.0 MeV have been measured with uncertainties of 1–3% and energy resolution between 30 and 100 keV. Some fine structure is evident, especially for the higher mass numbers. If one ignores the fine structure, the position of the cross section maximum increases in energy and the overall magnitude of the cross section increases slightly as the mass number increases. A neutron-excess dependent optical potential which fits 1.0 MeV differential scattering cross sections, with an added standard energy dependence, reproduces these trends and fits the cross sections within 5% below 2 MeV, indicating that the low energy total cross sections of the tin isotopes are consistent with a neutron-excess

dependent spherical optical model.

These cross sections provide an accurate means for normalizing low-energy neutron scattering differential cross sections of these isotopes. This method leads to an uncertainty in normalization about half as large as that resulting from the conventional use of known carbon or hydrogen differential scattering cross sections.

ACKNOWLEDGMENTS

The authors wish to acknowledge many useful discussions with Professor M. T. McEllistrem, in addition to his critical reading of the manuscript and general support. This work was partially supported by the National Science Foundation under Grant No. PHY 78-03209A02.

*Present address: Los Alamos Scientific Laboratory, Los Alamos, NM 87545.

†Present address: c/o Schlumberger Middle East. S. A., P.O. Box 21, Abu Dhabi, United Arab Emirates.

¹R. Graetzer, S. M. Cochick, and J. X. Saladin, Phys. Rev. C **12**, 1462 (1975).

²P. H. Stelson, F. K. McGowan, R. L. Robinson, and W. T. Milner, Phys. Rev. C **2**, 2015 (1970).

³R. W. Finlay, J. Rapaport, M. H. Hadizadeh, M. Mirzaa, and D. E. Bainum, Nucl. Phys. **A338**, 45 (1980).

⁴W. Makofske, W. Savin, H. Ogata, and T. H. Kruse, Phys. Rev. **174**, 1429 (1968).

⁵G. R. Satchler, *Isospin in Nuclear Physics*, edited by D. H. Wilkinson (North-Holland, Amsterdam, 1969).

⁶J. C. Ferrer, J. D. Carlson, and J. Rapaport, Nucl. Phys. **A275**, 325 (1977).

⁷J. Rapaport, V. Kulkarni, and R. W. Finlay, Nucl. Phys. **A330**, 15 (1979).

⁸J. Lachkar, M. T. McEllistrem, G. Hauout, Y. Patin, J. Sigaud, and F. Cocu, Phys. Rev. C **14**, 933 (1976).

⁹J. Rapaport, T. S. Cheema, D. E. Bainum, R. W. Finlay, and J. D. Carlson, Nucl. Phys. **A313**, 1 (1979).

¹⁰J. Rapaport, M. Mirzaa, H. Hadizadeh, D. E. Bainum, and R. W. Finlay, Nucl. Phys. **A341**, 56 (1980).

¹¹Isotope samples loaned by Stable Isotopes Division and J. Harvey, Oak Ridge National Laboratory.

¹²J. L. Weil, T. W. Godfrey, and R. W. Harper, Bull. Am. Phys. Soc. **24**, 658 (1979).

¹³R. W. Harper, J. D. Brandenberger, and J. L. Weil, Phys. Rev. C (to be published); R. W. Harper, J. L. Weil, and J. D. Brandenberger, Bull. Am. Phys. Soc.

22, 922 (1977); R. W. Harper, M. T. McEllistrem, and J. L. Weil, *ibid.* **24**, 854 (1979).

¹⁴R. K. Adair, Rev. Mod. Phys. **22**, 249 (1950).

¹⁵D. W. Miller, R. K. Adair, C. K. Bockelman, and S. E. Darden, Phys. Rev. **88**, 83 (1952).

¹⁶D. I. Garber and R. R. Kinsey, Brookhaven National Laboratory Report No. BNL 325, 1976, Vol. II.

¹⁷J. Cochran, M. S. thesis, University of Kentucky, 1974 (unpublished).

¹⁸L. V. Spencer and S. Woolf, Nucl. Instrum. Methods **97**, 567 (1971).

¹⁹F. D. McDaniel, J. D. Brandenberger, G. P. Glasgow, and H. G. Leighton, Phys. Rev. C **10**, 1087 (1974).

²⁰William Galati, Ph.D. dissertation, University of Kentucky, 1969 (unpublished).

²¹F. G. Perey, T. A. Love, and W. E. Kinney, Oak Ridge National Laboratory Report No. ORNL 4823, 1972 (unpublished).

²²R. B. Schwartz, R. A. Schrack, and H. T. Heaton II, National Bureau of Standards Monograph 138, 1974 (unpublished).

²³J. F. Whalen, Argonne National Laboratory Report No. ANL 7210, 1966 (unpublished).

²⁴K. K. Seth, Phys. Lett. **16**, 306 (1965).

²⁵J. Harvey, personal communication.

²⁶D. G. Foster and D. W. Glasgow, Phys. Rev. C **3**, 576 (1971).

²⁷C. M. Perey and F. G. Perey, At. Data Nucl. Data Tables **17**, 1 (1976).

²⁸D. Wilmore and P. E. Hodgson, Nucl. Phys. **55**, 673 (1964).